

Polycrystalline materials in $\text{MoO}_3\text{-ZrO}_2\text{-V}_2\text{O}_5$ system

M. Markova-Velichkova · R. Iordanova ·
A. Stoyanova · Y. Dimitriev · D. Klissurski

Received: 12 June 2006 / Accepted: 9 November 2006 / Published online: 27 March 2007
© Springer Science+Business Media, LLC 2007

Abstract Melt quenching technique was applied to study tendency for phase formation and amorphization in the $\text{MoO}_3\text{-ZrO}_2\text{-V}_2\text{O}_5$ system. By X-ray diffraction were detected the main crystalline phases separated during the quenching: $\text{Zr}(\text{MoO}_4)_2$, V_2MoO_8 , $(\text{Mo}_{0.3}\text{V}_{0.7})_2\text{O}_5$, $\text{V}_{0.95}\text{Mo}_{0.97}\text{O}_5$ but in a wide concentration range the dominant crystalline phase was monoclinic ZrO_2 . The average particle sizes of the obtained crystal phases were in the range 30–50 nm. A narrow glass formation area was situated, near $\text{MoO}_3\text{-V}_2\text{O}_5$ side. The glass-crystalline samples were obtained in the MoO_3 - and V_2O_5 -rich compositions. The phase formation was proven by IR analysis also. IR data showed that the main structural units built up the glass network are corner shared VO_5 and MoO_6 groups while in the corresponding crystal V_2MoO_8 phase MeO_6 ($\text{Me} = \text{V}, \text{Mo}$) octahedra are corner and edge shared (band at 580 cm^{-1}).

Introduction

A family of materials with general formulas AM_2O_7 and AM_2O_8 ($\text{A} = \text{Zr}, \text{Hf}$; $\text{M} = \text{V}, \text{Mo}, \text{W}$) has been shown to exhibit negative thermal expansion (NTE) over a wide temperature range [1–4]. The use of these materials in composites facilitates the control of bulk thermal expansion properties. Zero, or close to zero, thermal expansion is needed for various applications in optics, electronics and other fields where exact positioning of parts is crucial [5, 6]. At present several processes such as solid state reaction, sol-gel method and coprecipitation route were employed for preparation of these materials [7–10]. Their choice is very important for the design of structural features, properties and potential applications. The object of our investigation is the $\text{MoO}_3\text{-ZrO}_2\text{-V}_2\text{O}_5$ system. The phase diagrams of binary $\text{V}_2\text{O}_5\text{-ZrO}_2$ [11], $\text{MoO}_3\text{-ZrO}_2$ [12] and $\text{MoO}_3\text{-V}_2\text{O}_5$ [13] systems are known. In these systems exist two incongruent melting compounds $\text{Zr}(\text{MoO}_4)_2$ and ZrV_2O_7 and one congruent melting phase V_2MoO_8 . Low melting eutectic were situated near MoO_3 and V_2O_5 corner. In the literature there are no data for phase formation in the ternary $\text{MoO}_3\text{-ZrO}_2\text{-V}_2\text{O}_5$ system. The main task in this study is to investigate tendency for phase formation by melt quenching technique.

M. Markova-Velichkova (✉) · R. Iordanova ·
D. Klissurski
Institute of General and Inorganic Chemistry, Bulgarian
Academy of Sciences, 1113 Sofia, Bulgaria
e-mail: markova@svr.igic.bas.bg

A. Stoyanova
Department of Chemistry and Biochemistry, Medical
University, 5800 Pleven, Bulgaria

Y. Dimitriev
University of Chemical Technology and Metallurgy, 1756
Sofia, Bulgaria

Experimental

All batches were prepared using reagent-grade ZrO_2 , MoO_3 and V_2O_5 in different molar ratio. The homogenized batches were melted for 10 min in silica crucibles under air in the temperature range up to $1300\text{ }^\circ\text{C}$.

The melting temperature were chosen taking into account the liquids temperatures in the binary ZrO_2 – V_2O_5 , ZrO_2 – MoO_3 and MoO_3 – V_2O_5 systems, the peritectic temperature of decomposition of ZrV_2O_7 and $Zr(MoO_4)_2$ and the melting point of V_2MoO_8 [11–13]. Selected compositions on the right side of ZrV_2O_7 – $Zr(MoO_4)_2$ line were melted. The melts were quenched at high cooling rates, 10^4 – 10^5 K/s using roller-quenching technique. By this method only fragmented 1–5 mm flat pieces, about 50–100 μ m thick were obtained. Three sets of compositions were selected with constant ZrO_2 content (10, 20, and 30 mol.%) as well the compositions situated on ZrV_2O_7 – $Zr(MoO_4)_2$ and ZrO_2 – V_2MoO_8 lines. The phase formations were detected using X-ray diffraction and infrared spectroscopy (IR). Powder XRD patterns of the samples were registered with Philips APT 15 diffractometer at room temperature using Cu- K_{α} radiation in the $10^\circ < 2\theta < 80^\circ$ range. The average crystallite sizes of monoclinic ZrO_2 , trigonal $Zr(MoO_4)_2$ and V_2MoO_8 were calculated using Scherrer's equation. Differential thermal analysis were performed on DTA, Stanton Redcroft at a heating rate of 10 $^\circ$ C/min. Error bar of DTA curves, ± 5 $^\circ$ C. Fourier transform infrared experiments were carried out with Nicolet-320 (FTIR) spectrometer at a resolution of ± 1 cm^{-1} , by collecting 64 scans in the range 1200–400 cm^{-1} . Infrared spectra of all samples were obtained at room temperature using standard KBr pellet technique. The samples were mixed with dried KBr and pressed under vacuum.

Results and discussion

Figure 1 shows the investigated samples according to their nominal compositions. The glass formation area is situated near MoO_3 – V_2O_5 side up to 10 mol% ZrO_2 . Figure 2 (a–c) presents XRD patterns of compositions

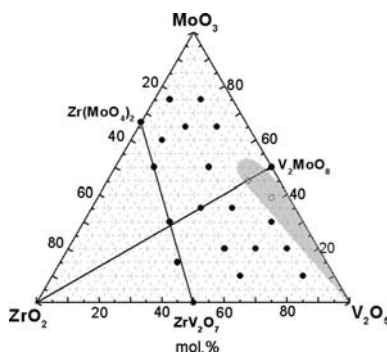


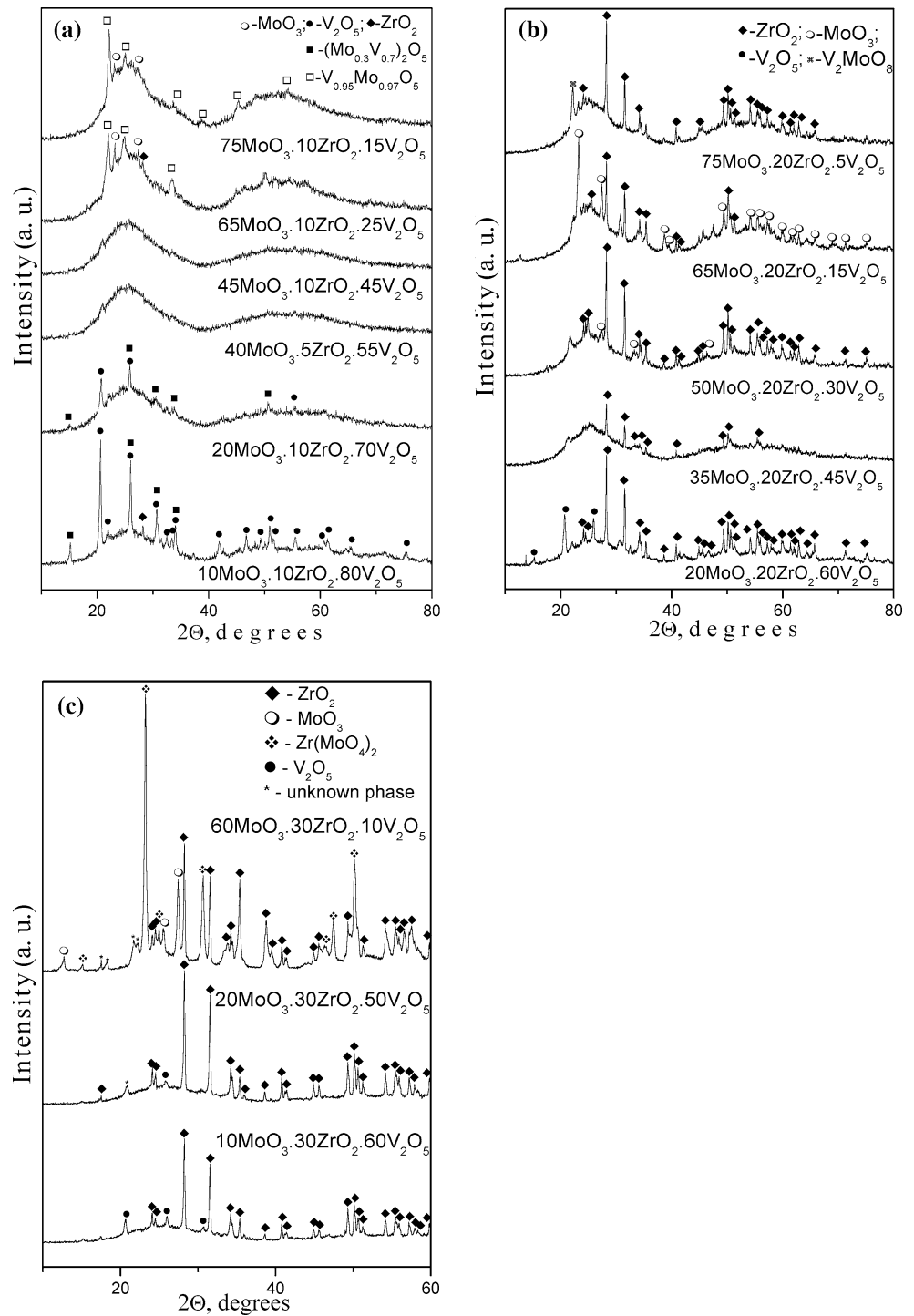
Fig. 1 Location of the investigated samples with their nominal composition in MoO_3 – ZrO_2 – V_2O_5 ternary system

with a constant ZrO_2 content (10, 20, 30 mol.%) whereas the MoO_3 concentration replaces V_2O_5 . All samples contain amorphous and crystalline phases. The compositions with 10 mol% ZrO_2 and a high V_2O_5 content (70–80 mol.%) contain $(Mo_{0.3}V_{0.7})_2O_5$ solid solution (JCPDS-21-0576), V_2O_5 (JCPDS-86-2248) and ZrO_2 (JCPDS-88-2390), (Fig. 2a). $V_{0.95}Mo_{0.97}O_5$ (JCPDS-77-0649) solid solution and MoO_3 (JCPDS 35-0609) crystals were detected in the samples rich in MoO_3 , (Fig. 2a). The X-ray diffraction patterns of $45MoO_3 \cdot 10ZrO_2 \cdot 45V_2O_5$ and $45MoO_3 \cdot 5ZrO_2 \cdot 55V_2O_5$ compositions are typical for the pure glass sample. A monoclinic ZrO_2 (JCPDS-88-2390) was the main crystalline phase formed in the compositions with 20 and 30 mol.% ZrO_2 (Fig. 2 b, c). In addition $Zr(MoO_4)_2$ phase (JCPDS-38-1466) crystallized in the sample rich in MoO_3 (60 mol.%), (Fig. 2c). In the compositions situated along the ZrV_2O_7 – $Zr(MoO_4)_2$ line, $Zr(MoO_4)_2$ (JCPDS-38-1466) and m- ZrO_2 (JCPDS-88-2390) crystallized from the melts (Fig. 3). ZrO_2 and V_2MoO_8 (JCPDS-74-1510) crystallized after slow cooling of the $45MoO_3 \cdot 10ZrO_2 \cdot 45V_2O_5$ melt composition. The same phases (ZrO_2 and V_2MoO_8) were separated in other samples situated on the same ZrO_2 – V_2MoO_8 line (Fig. 4). The obtained crystalline phases m- ZrO_2 , $Zr(MoO_4)_2$ and V_2MoO_8 during the fast quenching are characterized with small particle size. The average dimensions are in the range of 30–50 nm. New binary or ternary compounds were not detected in XRD patterns of all investigated compositions.

DTA curves of selected compositions situated on ZrO_2 – V_2MoO_8 line (Fig. 5) possess two endothermic peaks at 520 and at about 600 $^\circ$ C. As the first peak is at the same temperature (520 $^\circ$ C) obviously it corresponds to the solidus temperature. The shape of the DTA curves is typical for the system of simple eutectic type.

The IR spectra confirmed obtained XRD data. The high intensity band at 780 cm^{-1} along with the weak band at 940 cm^{-1} in the spectrum of $50MoO_3 \cdot 37.5ZrO_2 \cdot 12.5V_2O_5$ composition are typical for the vibration of MoO_4 structural units building trigonal $Zr(MoO_4)_2$ [14], (Fig. 6). The characteristic bands of pure V_2O_5 (1010, 820, 600, 480 cm^{-1}), [15, 16] and m- ZrO_2 (740 cm^{-1} and bands below 600 cm^{-1}) [17] were observed in the spectrum of $15MoO_3 \cdot 47.5ZrO_2 \cdot 37.5V_2O_5$. The spectrum of crystallized $45MoO_3 \cdot 10ZrO_2 \cdot 45V_2O_5$ sample is typical for the vibrations of MoO_6 and VO_6 units building V_2MoO_8 crystal structure [18, 19]. In the spectrum of the same composition in glass state absent the band at 580 cm^{-1} corresponds to the edge shared octahedra [20].

Fig. 2 XRD patterns of the compositions with a constant ZrO₂ content: **(a)** 10 mol.% ZrO₂; **(b)** 20 mol% ZrO₂; **(c)** 30 mol% ZrO₂.



ZrO₂ precipitates in a wide concentration range because above the peritectic line in the binary phase diagrams co-existent phases are ZrO₂ and a liquid [11, 12]. It was not proven presence of ternary compound. Because of the high cooling rates there is not enough time for the crystal growth and small crystallites were formed due to the high nucleation rate. In this manner it is possible to achieve submicron size distribution of

the particles. That is way the applied melt quenching method may be considered as an appropriate one to preparation of polycrystalline materials with controlled particle size distribution. The XRD, DTA and IR data allow us to suggest that ZrO₂–V₂MoO₈ line is a real section in the MoO₃–ZrO₂–V₂O₅ system following the rules for the building up the equilibrium phase diagram [21]. The situation of the glass formation region near

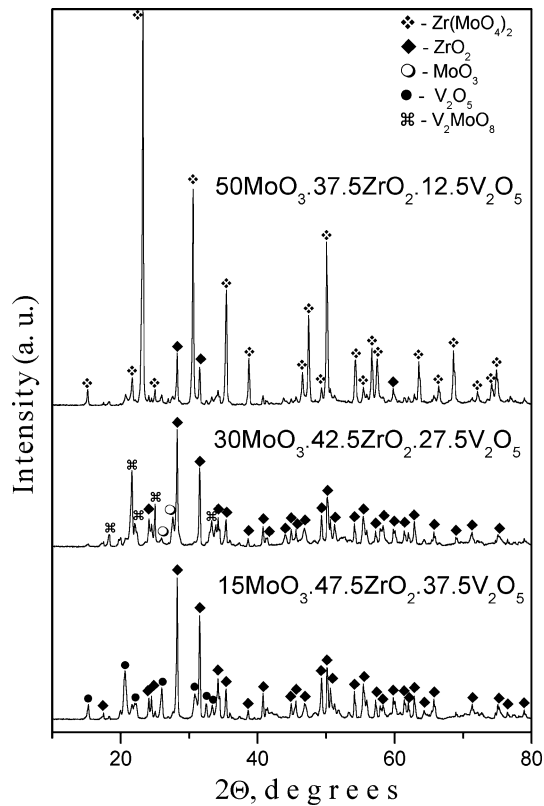


Fig. 3 XRD patterns of the compositions on ZrV_2O_7 – $Zr(MoO_4)_2$ line

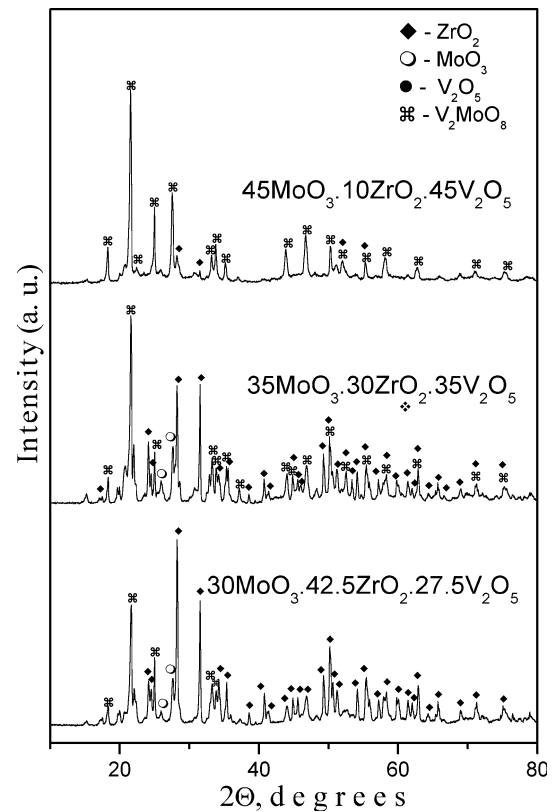


Fig. 4 XRD patterns of the compositions on ZrO_2 – V_2MoO_8 line

the V_2O_5 – MoO_3 side confirms our previous studies that these oxides are conditional glass formers [22]. From structural point of view the reason for amorphization of some compositions can be that during the cooling of the melts edge share between the polyhedra was not realized. The absence of this kind of linkages was proven by IR spectra. Instead of that MoO_6 and VO_5 polyhedra are corner shared (bands above 800 cm^{-1}) which is one of the main criteria for the improvement of glass formation ability [22, 23]. ZrO_2 acts as a modifier and increases the crystallization ability of the melts above 10 mol.%. That is way the vetrification of the samples and their additional short time heat treatment is another possibility to control the crystallization processes and especially the particle size.

Conclusion

It is established that in a wide concentration range in MoO_3 – ZrO_2 – V_2O_5 system crystallized mainly monoclinic ZrO_2 . $Zr(MoO_4)_2$ crystallized in compositions rich in MoO_3 . The ZrO_2 – V_2MoO_8 line may be considered as a real quasi–binary section. The glass formation region is situated near V_2O_5 – MoO_3 side and it

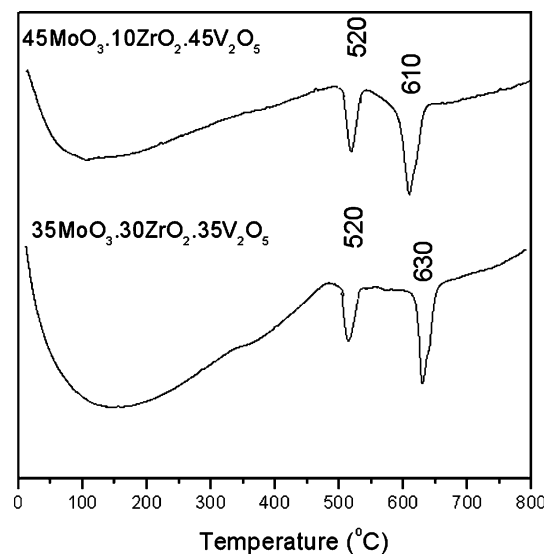


Fig. 5 DTA curves of composition on ZrO_2 – V_2MoO_8 line

is confirmed that these compounds are the network former. It is proven that the melt quenching technique is an appropriate for the preparation of polycrystalline materials with small particle size distribution.

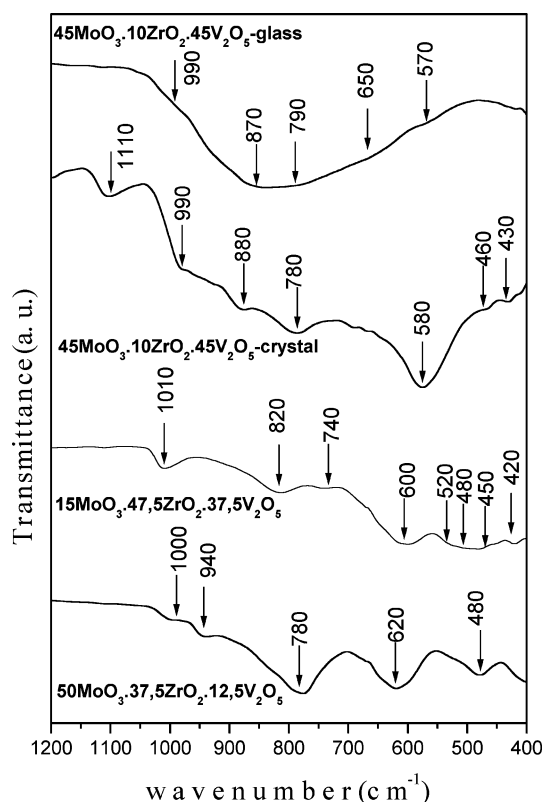


Fig. 6 IR spectra of the selected compositions

Acknowledgments This work was financial supported by contract 25/2006, Medical University, Pleven, Bulgaria

References

1. Evans JSO, Mary TA, Vogt T, Subramanian MA, Sleight AW (1996) Chem Mater 8:2809

2. Mary TA, Evans JSO, Vogt T, Sleight AW (1996) Science 272:90
3. Evans JSO, Hanson PA, Ibbreson RM, Duan N, Kameswari U, Sleight AW (2000) J Am Chem Soc 122:8694
4. Zhang SY, Zhao XH, Ma H, Wu XY (2000) Chin J Chem 18:571
5. Sega K, Koroda Y, Sakata H (1998) J Mater Sci 33:1303
6. Christodoulakis A, Machli M, Lemonidou A, Boghosian S (2004) J Catal 222: 293
7. Samaranch B, Ramirez De La Piscina P, Clet G, Houalla M, Homs N (2006) Chem Mater. 18:1581
8. Allen S, Ward RJ, Hampson MR, Gover RKB, Evans JSO (2004) Acta Cryst B60:32
9. Andersen AMK, Carlson S (2001) Acta Cryst B57:20
10. Craig DF, Hummel FA (1972) J Am Chem Soc 55:532
11. Roth R, Worin J (1959) J Res Natl Bur Standarts 61:1
12. Mohosoev MV, Bazarova JG (1990) Complex oxides of Molybdenum and Tungsten with oxides of I–IV group elements. Nauka, Moskow p 215
13. Fotiev A, Slobodin B, Hodos M (1988) Vanadates—composition, synthesis, structure, properties, Nauka, Moskow, p 75
14. Muthu DVS, Chen B, Wrobel JM, Andersen AMK, Carlson S, Kruger MB (2002) Phys Rev B65:64101
15. Bachmann HG, Ahmed FR, Barnes WH (1961) Z Krist 115:110
16. Abello L, Husson E, Repelin Y, Lucazeau G (1983) Spectrochimica Acta 39A:641
17. Mondal A, Ram S (2004) J Am Ceram Soc 87:2187
18. Eick HA, Kilbirg L (1966) Acta Chem Scand 20:1658
19. Bielanski A, Dyrek K, Pozniczek J, Wenda E (1973) Commun. of the Department of Chemistry (in Bulgaria) 2 p 531
20. Seguin L, Figlarz M, Cavagnat R, Lassegues J (1995) Spectrochim Acta. A51:1323
21. Zaharov AM (1978) Phase diagrams of binary and ternary systems. Moskow, Metallurgy (in Russian)
22. Iordanova R, Dimitrov V, Dimitriev Y, Klissurski D (1994) Non-Cryst Solids 108:58
23. Gupta P (1993) J Am Ceram Soc 76(5):1088